

# OPTICAL COHERENCE TOMOGRAPHIC IMAGING OF HUMAN TISSUE AT 1.55 $\mu$ M AND 1.81 $\mu$ M USING ER- AND TM-DOPED FIBER SOURCES

Brett E. Bouma, Lynn E. Nelson, Guillermo J. Tearney, David J. Jones,  
Mark E. Brezinski,\* and James G. Fujimoto

Massachusetts Institute of Technology, Department of Electrical Engineering and Computer Science  
and Research Laboratory of Electronics, Cambridge, Massachusetts 02139; \*Also with  
Massachusetts General Hospital, Boston, Massachusetts 02114

(Paper JBO/IB-014 received Sep. 4, 1997; revised manuscript received Oct. 1, 1997; accepted for publication Oct. 7, 1997.)

## ABSTRACT

We demonstrate two short-coherence-length, rare-earth-doped fiber optical sources for performing optical coherence tomography (OCT) in human tissue. The first source is a stretched-pulse, mode-locked Er-doped fiber laser with a center wavelength of 1.55  $\mu$ m, a power of 100 mW, and a bandwidth of 80 nm. The second is a Tm-doped silica fiber fluorescent source emitting up to 7 mW of power at 1.81  $\mu$ m with a bandwidth of 80 nm. The OCT imaging depth of penetration in *in vitro* human aorta is compared using these sources and conventional 1.3- $\mu$ m sources. © 1998 Society of Photo-Optical Instrumentation Engineers. [S1083-3668(98)00201-9]

**Keywords** interferometry in biomedicine; imaging; optical coherence tomography; fiber optics.

## 1 INTRODUCTION

There is significant interest currently in developing short-coherence-length, high-powered light sources for performing optical biopsies, the noninvasive visualization of tissue structural morphology. Optical coherence tomography (OCT)<sup>1</sup> utilizes such a source to localize backscattering sites within a sample using coherence domain ranging.<sup>2,3</sup> Several optical sources have been used for performing OCT in human tissue, including superluminescent diodes (SLD),<sup>1</sup> fluorescence from organic dye<sup>4</sup> and solid-state<sup>5</sup> laser media, mode-locked solid-state lasers,<sup>6,7</sup> and Nd-doped fiber fluorescence.<sup>8</sup>

Parameters relevant to the evaluation of sources for performing OCT include center wavelength, optical bandwidth, average optical power, and spatial coherence. Since OCT uses focusing to achieve transverse localization, the optical source must have a high degree of spatial coherence. High average power ensures a sufficient rate of singly scattered photons returning from within a turbid sample. The optical bandwidth of the source determines the axial resolution; broader bandwidth sources are able to resolve smaller axial dimensions. Finally, since the scattering and absorption cross sections for biological tissue are wavelength dependent, different wavelength sources will have different penetration depths. Although a systematic

study of the center wavelength dependence of contrast and depth of penetration in OCT imaging has not been performed, a qualitative comparison has shown significantly deeper imaging depth using 1.3- $\mu$ m sources relative to 0.8- $\mu$ m sources.<sup>9</sup> This is not surprising since in this wavelength range the primary attenuation mechanism for back-reflected light is scattering. At longer wavelengths, where water and other cellular constituents exhibit significant absorption, it is expected that the primary attenuation mechanism will shift from scattering to absorption.

These criteria explain why mode-locked solid-state lasers have been shown to provide superior performance in OCT imaging systems.<sup>6,7</sup> The clinical implementation of OCT, however, requires the additional considerations of source economy and simplicity. Mode-locked solid-state lasers suffer under these more stringent concerns, which favor semiconductor sources and diode-pumped rare-earth-doped fiber sources. In this study we present OCT imaging with rare-earth-doped fiber sources at wavelengths of 1.55 and 1.81  $\mu$ m, and demonstrate that these longer wavelengths allow significant imaging penetration into biological tissue.

Address all correspondence to Jame G. Fujimoto.

1083-3668/98/\$10.00 © 1998 SPIE

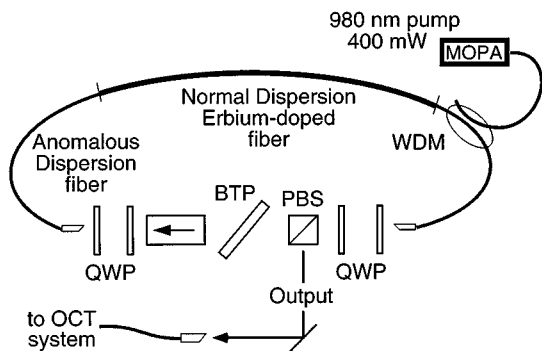


**Fig. 1** Schematic representation of the stretched-pulse Er-doped fiber laser. MOPA, master oscillator power amplifiers; WDM, wavelength-division multiplexer; QWP, quarter wave plate; PBS, polarizing beam splitter; BTP, tuning plate.

## 2 METHODS

The Er-doped fiber source (EDFS) used in this experiment was a stretched-pulse fiber ring laser mode locked by nonlinear polarization rotation.<sup>10</sup> These lasers are capable of producing pulse durations as low as 70 fs, with spectra centered at 1.55  $\mu\text{m}$ . The stretched-pulse laser is composed of segments of alternately large normal and anomalous dispersion fiber (shown in Figure 1), which causes the pulse to be repeatedly stretched and compressed during propagation around the resonator. Construction of the cavity with an air gap and bulk waveplates allows the output to be extracted where the pulses have the highest energy and broadest bandwidth.<sup>11</sup> An average output power of 100 mW was obtained with 400 mW of pump power from a commercial 980-nm, semiconductor master oscillator/power amplifier.

Owing to the placement of the output coupling port of the laser immediately after the positive-dispersion Er-doped fiber, the pulses emitted from the laser have a positive frequency sweep or chirp. This means that as the output pulses propagate within standard telecommunications optical fibers, the anomalous dispersion they experience leads to pulse compression and self-phase modulation. To avoid the spectral reshaping that results from this self-phase modulation, we attenuated the output from the laser to 15 mW before recoupling the pulses to our fiber optic delivery system. It is also possible to avoid self-phase modulation external to the resonator while utilizing nearly the full power provided by this laser by reversing the sign of the chirp with a grating-based dispersive delay line. For the purpose of OCT imaging, however, an average power of 15 mW was sufficient.

The spectrum of the light from the mode-locked EDFS, centered at 1.55  $\mu\text{m}$ , is shown in Figure 2. Since the axial point spread function in OCT is determined by the Fourier transform of the source power spectrum, the sharp edges of the EDFS spectrum are undesirable. The near-rectangular spec-

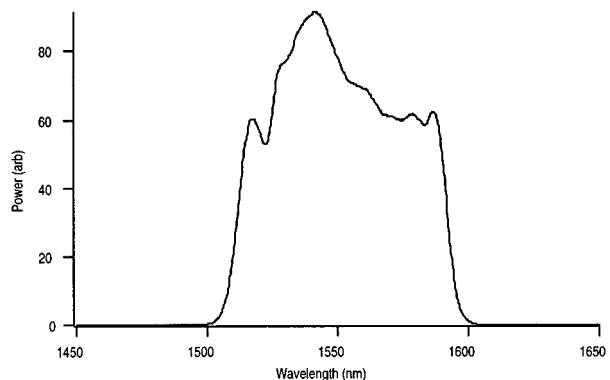


**Fig. 2** Optical power spectrum produced by the stretched-pulse, Er-doped fiber laser.

trum, in this case, gives rise to a sinc-like axial response. In an OCT image, this artifact will be observed as a ghost above and below sites of strong back-reflection. The full-width half-maximum (FWHM) of the Fourier transform of the EDFS power spectrum, and hence the axial resolution of an OCT system based on this source, is 17  $\mu\text{m}$ .

To explore OCT imaging with a source wavelength near 1.8  $\mu\text{m}$ , we constructed a Tm-doped silica fiber fluorescent source (TDFS). Although mode locking of a Tm-doped fiber laser has been demonstrated,<sup>12,13</sup> the pulse spectrum achieved was not broader than 18 nm. Since the stretched-pulse concept is difficult to apply at a wavelength near 1.8  $\mu\text{m}$ , we used the broad spectral fluorescent emission of Tm-doped fiber directly. This source consists of a 1.3-m length of Tm-doped silica fiber, both ends of which were angle polished to suppress feedback. The TDFS is pumped by a 780-nm titanium sapphire laser at absorbed power levels as high as 350 mW. At an absorbed pump power of 350 mW, the amplified spontaneous emission output power was 7 mW. The broad, near-infrared absorption of Tm allows pump wavelengths throughout the range of 770 to 800 nm. This insensitivity to pump wavelength is favorable for excitation with semiconductor diode lasers.

Light output from the end of the TDFS opposite the pump laser was collimated, passed through an optical isolator, and coupled into an SMF-28 fiber optic jumper for delivery to the OCT imaging system. The optical isolator ensured that light back-reflected from the imaging system was prevented from reentering the Tm-doped fiber. A coupling loss of -7 dB was incurred, with transmission of 1.4 mW of power to the OCT system. The spectrum of this light (Figure 3) is centered at 1808 nm with a FWHM bandwidth of 80 nm. This bandwidth corresponds to an OCT axial resolution of 18  $\mu\text{m}$ .

The system used for OCT imaging with the two doped fiber sources was based upon a wavelength-independent fiber optic splitter (Gould Fiber Optics). This splitter was designed for symmetric

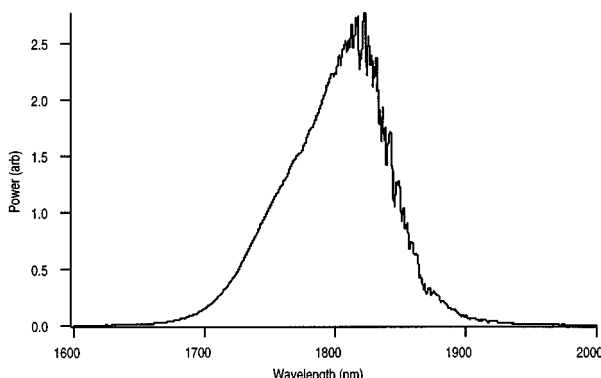


**Fig. 3** Optical power spectrum produced by the fluorescent Tm-doped fiber source.

power splitting at a center wavelength of  $1.3\text{ }\mu\text{m}$ . At both  $1.55\text{ }\mu\text{m}$  and  $1.8\text{ }\mu\text{m}$ , the split ratio was  $\sim 60/40$  and preserved the spectrum of both fiber sources. This allowed the same OCT system to be used for imaging at three different wavelengths ( $1.3$ ,  $1.55$ , and  $1.8\text{ }\mu\text{m}$ ) so that registration of the imaged cross section within a sample could be preserved. The time required for the acquisition of individual images was 6 s. Light from the sample arm of the splitter was collimated and then focused with an aspheric lens to a focal spot size of  $30\text{ }\mu\text{m}$ . The chromatic aberration of these optics was not significant over the spectral range of any one source, but the wavelength-dependent focal length change from  $1.3$  to  $1.8\text{ }\mu\text{m}$  required compensation. The use of two independent lenses for collimation and focusing is advantageous in this case, since the relative positioning of each lens can be used to maintain a constant focal spot diameter while switching between sources.

### 3 RESULTS

OCT images of an *in vitro* human aorta were obtained using the mode-locked EDFS. Since the power available from this source was sufficient to obtain high dynamic range imaging, we compared these images with those obtained using a mode-locked chromium-doped forsterite laser.<sup>7</sup> The spectral bandwidth of the forsterite laser was reduced so that the axial resolution obtained using this source was approximately equal to the  $17\text{-}\mu\text{m}$  resolution obtained with the EDFS. The signal-to-noise ratio (112 dB) and the transverse resolution ( $30\text{ }\mu\text{m}$ ) were adjusted to be equivalent for imaging with both sources. A comparison of two images acquired with these sources is shown in Figure 4 (Cr:forsterite laser source, upper image; EDFS, lower image). The sample was prepared within 24 h postexcision by opening the aorta and exposing the intima for direct imaging. The specimen was immersed in saline with only the intimal surface exposed to air. These images show approximately the same cross section and demonstrate equivalent depths of pen-

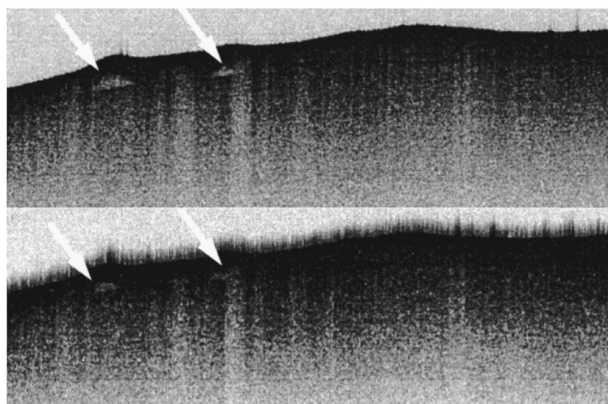


**Fig. 4** Comparison between images of an *in vitro* human aorta acquired with the  $1.55\text{-}\mu\text{m}$  Er-doped fiber laser source (bottom) and a  $1.3\text{-}\mu\text{m}$  chromium-doped forsterite laser source (top). The axial resolution ( $16\text{ }\mu\text{m}$ ), signal-to-noise ratio (112 dB), and transverse resolution ( $30\text{ }\mu\text{m}$ ) for each image were equivalent. The images span 6 by 2 mm.

etration at  $1.3$  and  $1.55\text{ }\mu\text{m}$ . Since our axial scan length was limited to an optical depth of approximately 2 mm, we were not able to image the junction between the media and the adventitia of this aorta specimen, which had a physical full thickness of 4 mm. We believe that the features denoted by arrows in the figures are fatty streaks, although this was not confirmed by histologic correlation. The ghosts above and below the sites of strong back-reflection in the image acquired with the EDFS are most pronounced at the tissue surface, but can also be seen throughout the depth of the cross section. While the EDFS provides sufficient average power to enable the rapid acquisition of high dynamic range images and can be seen to provide satisfactory resolution and imaging depth, a significant improvement of the spectral shape is required for optimal OCT imaging. Spectral reshaping external to the laser is possible, but the application of linear wavelength-dependent filters would result in diminished spectral bandwidth and axial resolution.

A second specimen of human aorta was obtained for imaging with the TDFS. Since the system's signal-to-noise ratio obtained with the TDFS was limited to 102 dB by coupling losses and by the quantum efficiency of the InGaAs photodetector, comparison images were acquired with a  $1.3\text{-}\mu\text{m}$  SLD. The axial resolution provided by this diode ( $16\text{ }\mu\text{m}$ ) was similar to the  $18\text{-}\mu\text{m}$  coherence length of the TDFS. The OCT system was adjusted so that the transverse resolution ( $30\text{ }\mu\text{m}$ ) and the signal-to-noise ratio (102 dB) were equivalent for both sources. Figure 5 shows an image of the second aorta specimen acquired with the TDFS (lower image) and an image of approximately the same cross section obtained with the SLD (upper image). The large, nearly rectangular feature in these images is a matrix and is associated with atherosclerosis. As one would predict based on the TDFS spectrum of

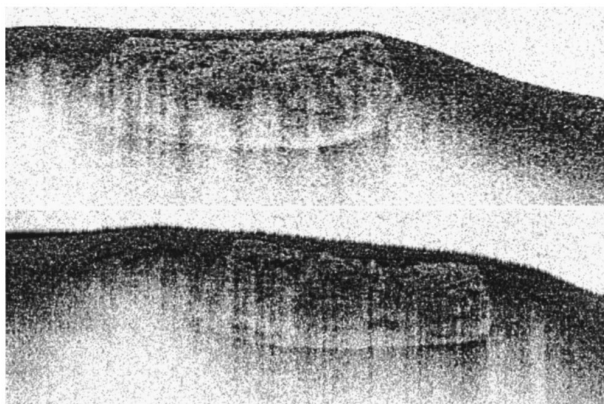


**Fig. 5** Comparison between images of a second *in vitro* human aorta specimen acquired with the 1.8- $\mu\text{m}$  Tm-doped fluorescent fiber source (bottom) and with a 1.3- $\mu\text{m}$  SLD (top). The axial resolution (18  $\mu\text{m}$ ), signal-to-noise ratio (102 dB), and transverse resolution (30  $\mu\text{m}$ ) for each image were equivalent. The images span 6 by 2 mm.

Figure 3, there are no appreciable ghost artifacts present in the image acquired at 1.81  $\mu\text{m}$ .

Comparison of the imaging depth of penetration provided by the TDFS and by the SLD yields a somewhat surprising result. Although the detailed scattering and absorption properties of human tissues in the 1- to 2- $\mu\text{m}$  spectral range are not known, it is expected that absorption is significantly larger at 1.8  $\mu\text{m}$  than at 1.3  $\mu\text{m}$ .<sup>14,15</sup> From this, one might infer that the imaging depth of penetration would be reduced at 1.8  $\mu\text{m}$  relative to 1.3  $\mu\text{m}$ . The OCT images in Figure 5, however, demonstrate a comparable imaging depth of penetration for the TDFS and for the SLD. This result can be understood by noting that while absorption may be stronger at 1.8  $\mu\text{m}$ , attenuation is also influenced by scattering. Since scattering should decrease with increasing wavelength, it is possible that the net change in attenuation between 1.3 and 1.8  $\mu\text{m}$  is small.

## 4 DISCUSSION

In conclusion, we have discussed the design and performance of two short coherence-length, rare-earth-doped fiber optical sources for performing OCT. We have applied these sources to the demonstration of OCT imaging at wavelengths between the primary water absorption bands (1.38 to 1.50  $\mu\text{m}$  and 1.9 to 2.2  $\mu\text{m}$ ) in the short-wavelength infrared spectral region. Although a systematic study of the optical properties of human tissue will be required for a detailed theoretical understanding of the depth of penetration for OCT imaging in this spectral region, the qualitative assessment presented indicates that doped-fiber sources at 1.55 and 1.8  $\mu\text{m}$  are well suited for OCT imaging.

## Acknowledgments

B. E. Bouma and L. E. Nelson are currently with the Wellman Laboratories of Photomedicine, Massa-

chusetts General Hospital, Boston, Massachusetts 02114, and Lucent Technologies, Bell Laboratories, Holmdel, New Jersey 07733, respectively. The authors thank Dr. E. Snitzer for donating the Tm-doped fiber. This research was sponsored in part by grants from the Office of Naval Research, Medical Free-Electron Laser Program, Grant N00014-94-1-0717; the National Institutes of Health, Contracts NIH-9-R01-EY11289-11 (JGF), NIH-9-R01-CA75289-01 (JGF and MEB), and NIH-1-R29-HL55686-01A1(MEB); the Air Force Office of Scientific Research, Grant F49620-95-1-0221; the Joint Services Electronics Program, Contract DAAH04-95-1-0038; and the U.S. Department of Commerce, Contract 70NANB6H0092.

## REFERENCES

- D. Huang, E. A. Swanson, C. P. Lin, J. S. Schuman, W. G. Stinson, W. Chang, M. R. Hee, T. Flotte, K. Gregory, C. A. Puliafito, and J. G. Fujimoto, "Optical coherence tomography," *Science* **254**, 1178–1181 (1991).
- R. C. Youngquist, S. Carr, and D. E. N. Davies, "Optical coherence domain reflectometry: a new optical evaluation technique," *Opt. Lett.* **12**, 158–160 (1987).
- K. Takada, I. Yokohama, K. Chida, and J. Noda, "New measurement system for fault location in optical waveguide devices based on an interferometric device," *Appl. Opt.* **26**, 1603 (1987).
- H.-H. Liu, P.-H. Cheng, and J. Wang, "Spatially coherent white-light interferometer based on a point fluorescent source," *Opt. Lett.* **18**, 678 (1993).
- X. Clivaz, F. Marquis-Weible, and R.-P. Salathe, R. P. Novak, and H. H. Gilgen, "High-resolution reflectometry in biological tissues," *Opt. Lett.* **17**, 4–6 (1992).
- B. Bouma, G. J. Tearney, S. A. Boppart, M. R. Hee, M. E. Brezinski, and J. G. Fujimoto, "High-resolution optical coherence tomography imaging using a modelocked Ti:Al<sub>2</sub>O<sub>3</sub> laser source," *Opt. Lett.* **20**, 1486–1488 (1995).
- B. E. Bouma, G. J. Tearney, I. P. Bilinsky, B. Golubovic, and J. G. Fujimoto, "Self-phase-modulated Kerr lens mode-locked Cr:Forsterite laser source for optical coherence tomography," *Opt. Lett.* **21**, 1839–1841 (1996).
- S. V. Chernikov, J. R. Taylor, V. P. Gapontsev, B. E. Bouma, and J. G. Fujimoto, "A 75-nm, 30-mW superfluorescent ytterbium fiber source operating around 1.06  $\mu\text{m}$ ," in *Conference on Lasers and Electro-Optics*, Vol. XI, paper CTuG8 in 1997 OSA Technical Digest Series, Optical Society of America, Washington, DC (1997).
- J. M. Schmitt, A. Knuttel, M. Yadlowsky, and M. A. Eckhaus, "Optical coherence tomography of a dense tissue: statistics of attenuation and backscattering," *Phys. Med. Biol.* **39**, 1705 (1994).
- H. A. Haus, K. Tamura, L. E. Nelson, and E. P. Ippen, "Stretched-pulse additive pulse modelocking in fiber ring lasers: theory and experiment," *J. Quantum Electron.* **31**, 591–598 (1995).
- K. Tamura, C. R. Doerr, L. E. Nelson, H. A. Haus, and E. P. Ippen, "Technique for obtaining high-energy ultrashort pulses from an additive-pulse mode-locked erbium-doped fiber ring laser," *Opt. Lett.* **19**, 46–48 (1994).
- L. E. Nelson, E. P. Ippen, and H. A. Haus, "Broadly tunable sub-500 fs pulses from an additive-pulse mode-locked thulium-doped fiber ring laser," *Appl. Phys. Lett.* **67**, 19–21 (1995).
- R. C. Sharp, D. E. Spock, N. Pan, and J. Elliot, "190-fs passively mode-locked thulium fiber laser with a low threshold," *Opt. Lett.* **21**, 881 (1996).
- J. L. Boulnois, "Photophysical processes in recent medical laser developments: a review," *Lasers Med. Sci.* **1**, 47 (1986).
- P. Parsa, S. L. Jacques, and N. S. Nishioka, "Optical properties of rat liver between 350 nm and 2200 nm," *Appl. Opt.* **28**, 2325–2327 (1989).